Electronic Supplementary Material (ESI) for Analyst.

Reaction Screening and Optimization of Atropine Synthesis in Continuous-Flow Guided by Preparative Electrospray

Caitlin E. Falcone[†,1], Zinia Jaman[†,1], Michael Wleklinski[1], Andy Koswara[2], David H. Thompson[*,1] R. Graham Cooks [*,1]

1Department of Chemistry, Purdue University, 560 Oval Drive, West Lafayette, IN 47907, USA

2Chemical Engineering, Purdue University, 480 W Stadium Ave, West Lafayette, IN 47907, USA

† These authors contributed equally to this work

List of contents

Microfluidics

Labtrix Start Flex (Chemtrix BV, Labtrix S1, Netherlands) employs custom fabricated parts made of PPS (polyphenylsulfide) and perfluoroelastomer. PPS provides excellent chemical resistance against hydrochloric acid, trifluoroacetic acid, nitrobenzene, acetic acid, sulfuric acid and butyl lithium. It can be used to perform syntheses at temperatures ranging from -20°C to +195°C and under pressures of up to 25 bar. The tube of the flex/ultraflex system is made from fluorinated ethylene propylene and the outer diameter is 1/32 inches and the inner diameter is 150µm. The microreactors were made of glass and differ in volume and number of connections. All staggered orientated microreactors (SOR) have width channel 300 µm and depth channel 120 µm. The sox SOR chips used were: 3221(three inlets and one outlet, volume 1µl), 3332 (three inlets and one outlet, volume 2µl), 3223 (three inlets and one outlet, volume 5µl), 3224 (four inlets and one outlet, volume 10+5µl), 3225 (four inlets and one outlet, volume 10µl), 3227 (three inlets and one outlet, volume 19.5µl). The Labtrix unit is enabled to pump five syringes with liquids into the micro reactor with a heating and cooling unit. All the gastight glass syringes were bought separately from Innovative Labor System. (ILS, Philadelphia, PA). The tubing and fittings connect the syringes with the selected connection port on the microreactor. All operations are controlled via ChemTrix GUI software, which is installed on a laptop and connected to the Labtrix S1 housing with a USB cable.

HPLC-MS Analysis

Separations were performed on an Agilent 1100 HPLC system (Palo Alto, CA) using a Varian C18 Amide column (3 µm, 150 x 2.1 mm id) and 10 uL injection volume. A binary mobile phase consisting of solvent systems A and B were used in gradient elution where A was 0.1% formic acid (v/v) in ddH_2O and B was 0.1% formic acid (v/v) in acetonitrile. The mobile phase flow rate was 0.3 mL/min. Initial conditions were set at 90:10 A:B with a linear gradient to 80:20 from 0 to 12 min, conditions were held at 80:20 from 12 to 18 minutes, followed by a linear gradient to 50:50 from 18 to 24 minutes and held at 50:50 until 30 minutes. Gradient conditions were reset to 90:10 A:B from 30 to 32 minutes, held the column equilibrated for 10 minutes at initial conditions prior to the next run. Following the separation, the column effluent was introduced by positive mode electrospray ionization (ESI) into an Agilent MSD-TOF mass spectrometer . The parameters were: ESI capillary voltage: 3.5 kV, nebulizer gas: nitrogen at 35 psi and350 °C, drying gas flow

rate: 9.0 L/min, fragmentor voltage: 165 V, skimmer: 60 V and OCT RF V: 250 V. Spectroscopic (UV at 280 nm) and mass data (from m/z 60-1000) were collected and analyzed using MassHunter software. The percent conversion was calculated as the product signal divided by the sum of all the peaks in the spectra.

RP-UPLC Analysis

An isocratic reverse-phase ultra-high performance liquid chromatography method (RP-UPLC) using the PATROL UPLC Process Analysis System (Waters Corp.) was developed to determine the yield of atropine reaction in continuous flow. The method was developed using ACQUITY BEH C18 (130 Å pore size, 1.7 µm particle size, 2.1 mm ID X 100 mm) as the stationary phase with potassium dihydrogen phosphate:methanol (80:20, v/v) at pH = 3.5 as the mobile phase. The mobile phase was prepared by dissolving potassium dihydrogen phosphate powder (Sigma-Aldrich, CAS: 7778-77-0) in HPLC-grade water (Fisher Scientific, CAS: 7732-18-5), which is pH-adjusted via titration using 85% orthophosphoric acid (Fisher Scientific, CAS: 7664-38-2,7732-18-5). The mobile phase flow rate through the column was 0.4 mL/min and the column temperature was maintained at 40 °C during the run. The detection of eluted atropine was accomplished using a dual-channel PDA detector at 190 and 225 nm in conjunction with ApexTrack analysis for integrating the atropine peak that was matched with an atropine standard chromatogram. Quantification was then performed via interpolation using a standard calibration curve at 225 nm. Three standard stock solutions of atropine sulfate were prepared by dissolving atropine sulfate powder (Sigma-Aldrich, CAS: 5908-99-6) in the mobile phase to generate concentrations of 1.20 mg/mL, 1.17 mg/mL, and 0.960 mg/mL. The solutions were used to generate three separate calibration curves by diluting the stock solutions inline to 1X, 2X, 4X, 8X, 16X, and 32X to cover a concentration range of 20-1200 µg/mL; the mean R^2 was 0.9997 (n=5). The mean slope of the curves was used for quantitation. The method's precision was calculated by repeated injections of the same standard solution without any change to the chromatographic methods.

Figure S1: Full scan MS of the preparative ES product of scheme 1a with HCl in water

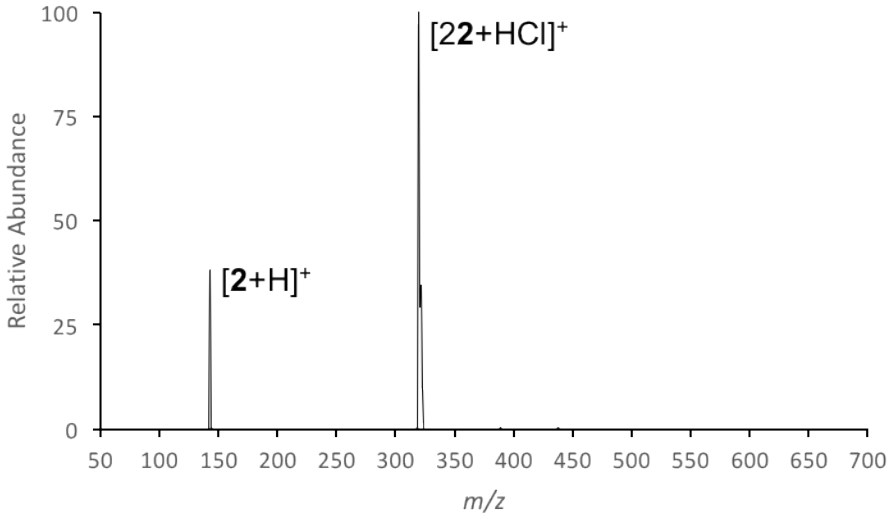

Full scan positive ion mode mass spectrum of the preparative ES product from the first step of the atropine synthesis with tropine, phenyl acetic acid and hydrochloric acid in water. In this sample *m/z* 142 $[\text{tropine+H}]^+$ and *m/z* 319 $[\text{2tropine + HCl}]^+$ are the most abundant ions.

Figure S2: Full scan MS of the preparative ES product of scheme 1a with HCl in dioxane

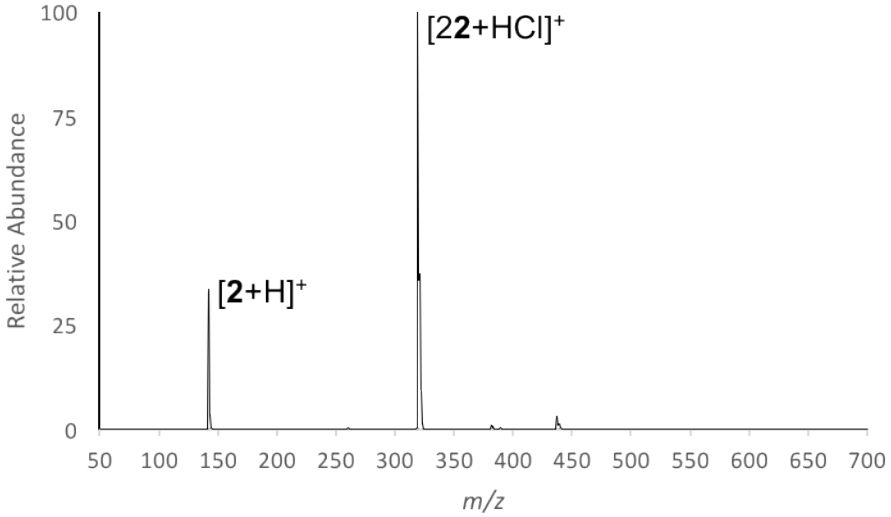

Full scan positive ion mode mass spectrum of the preparative ES product from the first step of the atropine synthesis with tropine, phenylacetic acid and hydrochloric acid in dioxane. In this sample *m/z* 142 $[\text{tropine +H}]^+$ and *m/z* 319 $[\text{2tropine + HCl}]^+$ are the most abundant ions.

Figure S3: Full scan MS of the preparative ES product of scheme 1b with DMA

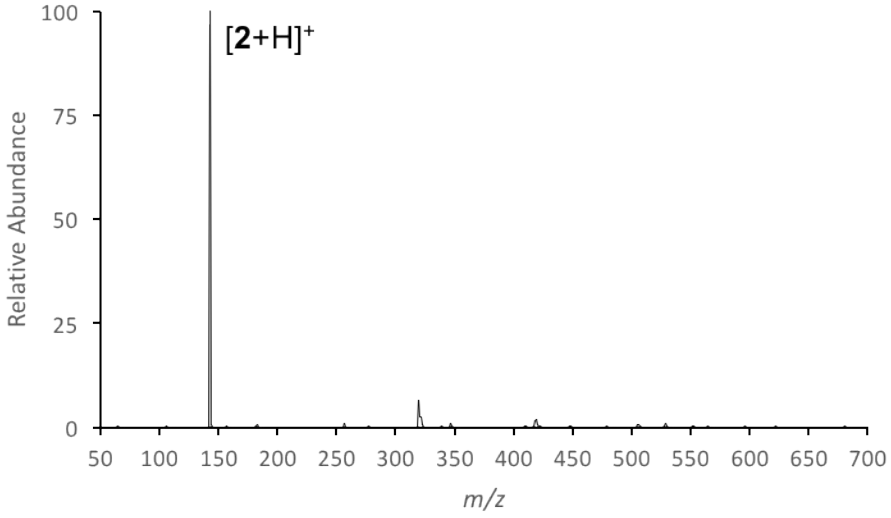

Full scan positive ion mode mass spectrum of the preparative ES product from the first step of the atropine synthesis with tropine and phenylacetic acid in DMA. In this sample *m/z* 142 [tropine +H]$^+$ is the most abundant ion.

Figure S4: Full scan MS of the preparative ES product of scheme 1c with HCl in dioxane

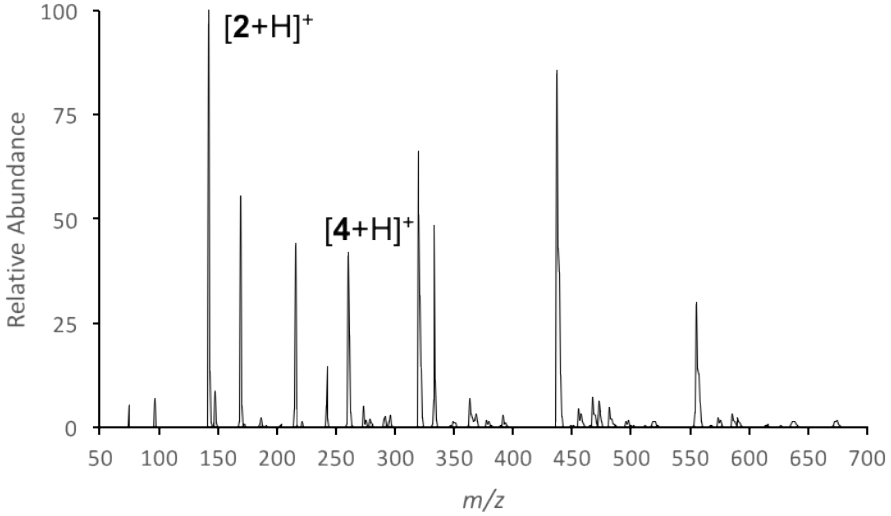

Full scan positive ion mode mass spectrum of the preparative ES product from the first step of the atropine synthesis with tropine, phenylacetyl chloride acid and hydrochloric acid in dioxane. In this sample *m/z* 142 [tropine +H]$^+$, *m/z* 260 [intermediate +H]$^+$, and *m/z* 319 [2tropine + HCl]$^+$ are present.

Figure S5: Full scan MS of the preparative ES product of scheme 1d with DMA

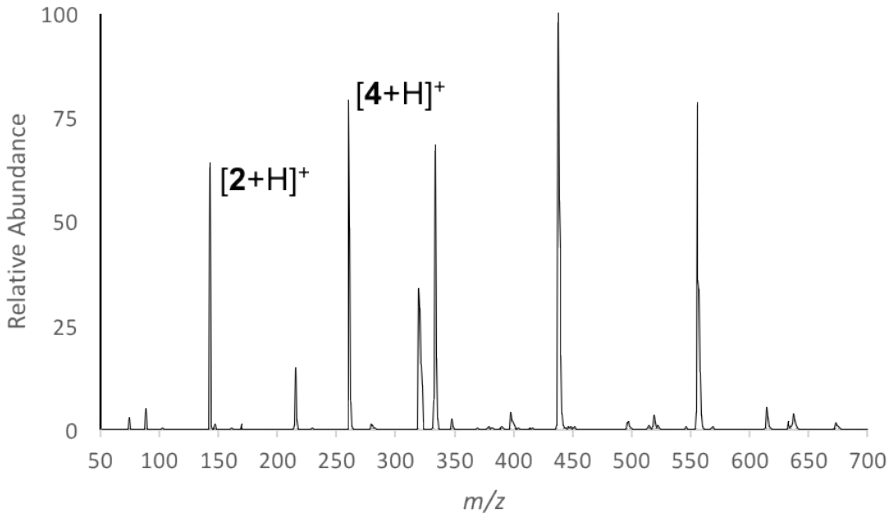

Full scan positive ion mode mass spectrum of the preparative ES product from the first step of the atropine synthesis with tropine, phenylacetyl chloride acid and hydrochloric acid in dioxane. In this sample *m/z* 142 $[\text{tropine}+H]^+$ and *m/z* 260 $[\text{intermediate}+H]^+$ are present.

Figure S6: Full scan MS of the preparative ES product of scheme 1d with DMF

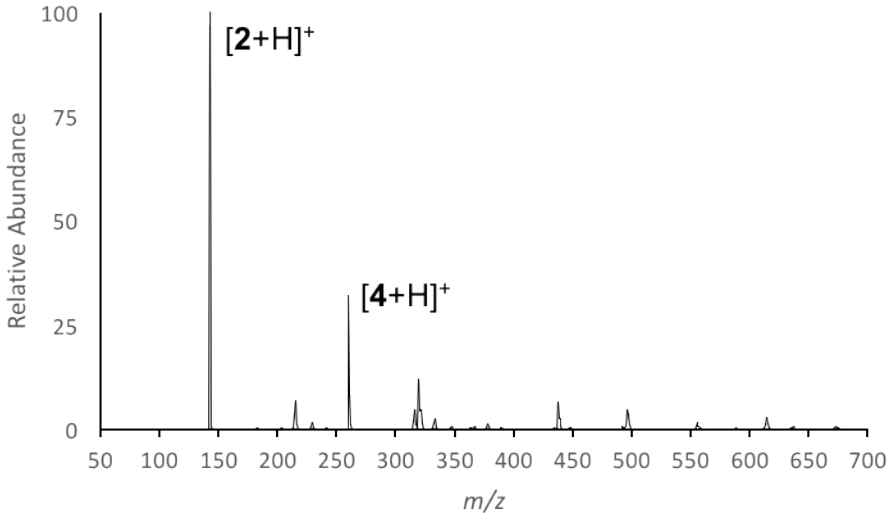

Full scan positive ion mode mass spectrum of the preparative ES product from the first step of the atropine synthesis with tropine and phenylacetyl chloride acid in DMF. In this sample *m/z* 142 $[\text{tropine}+H]^+$ and *m/z* 260 $[\text{intermediate}+H]^+$ are the most abundant ions.

Figure S7: Full scan MS of the preparative ES product of scheme 1d with ethanol

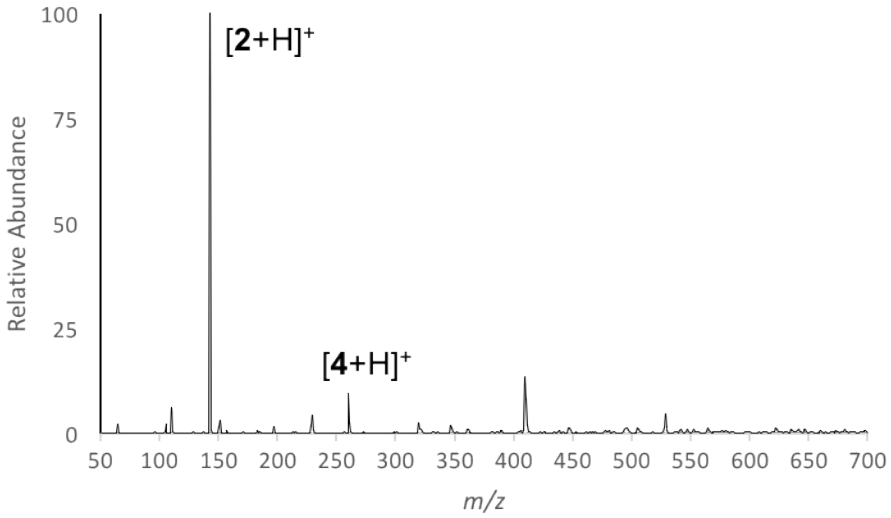

Full scan positive ion mode mass spectrum of the preparative ES product from the first step of the atropine synthesis with tropine and phenylacetyl chloride acid in ethanol. In this sample *m/z* 142 [tropine +H]$^+$ and *m/z* 260 [intermediate +H]$^+$ are present.

Figure S8: Full scan MS of the preparative ES product of scheme 1d with methanol

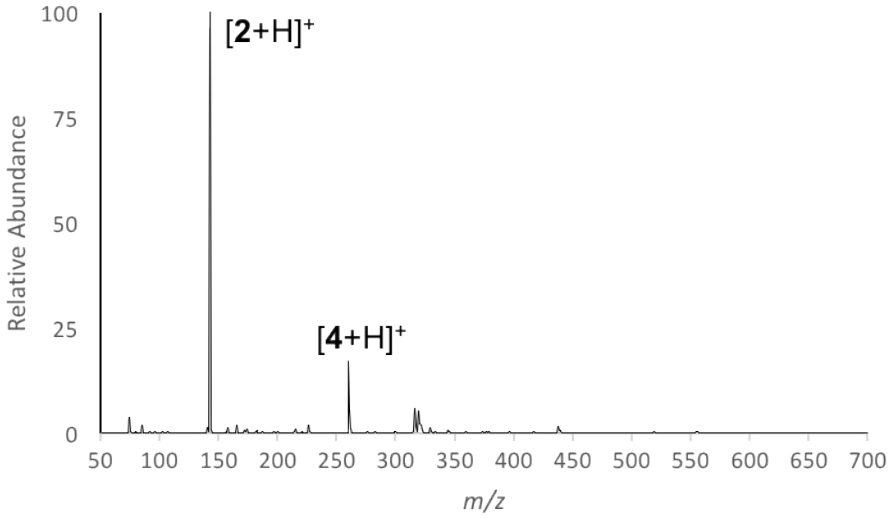

Full scan positive ion mode mass spectrum of the preparative ES product from the first step of the atropine synthesis with tropine and phenylacetyl chloride acid in methanol. In this sample *m/z* 142 [tropine +H]$^+$ and *m/z* 260 [intermediate +H]$^+$ are the most abundant ions.

Scheme S1: Byproducts during formation of intermediate **4**

Quaternary ammonium byproducts

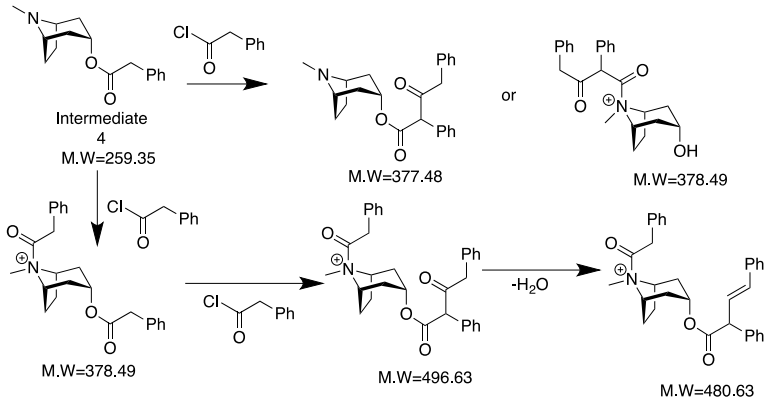

Byproducts associated with solvent DMF and DMA

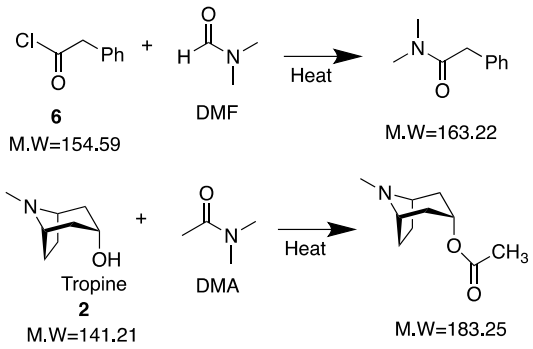

Table S1: Microfluidic synthesis of intermediate **4** using hydrochloric acid in dioxane

R1 Tropine (0.4M) µl/min	R2 HCl in dioxane (0.4M) µl/min	R3 Phenylacetyl chloride (0.4M) µl/min	R4 DMF µl/min	1st Residence time Tr_1min	2nd Residence time Tr_2 min	Temperature °C	Conversion of Intermediate (%) (by nESI-MS)
2.5	2.5	2.75	2.5	1	1.29	200	19.4
1.25	1.25	1.37	1.25	2	2.78	200	6.3
0.625	0.625	0.687	0.625	4	5.16	200	4.3
2.5	2.5	2.75	2.5	1	1.29	150	61.5
1.25	1.25	1.37	1.25	2	2.78	150	89.7
0.625	0.625	0.687	0.625	4	5.16	150	85.6
2.5	2.5	2.75	2.5	1	1.29	100	75.4
1.25	1.25	1.37	1.25	2	2.78	100	80.3
0.625	0.625	0.687	0.625	4	5.16	100	90.6

All reactions used the SOR 3224 chip (5+10 µl) and a pressure of 7 bar

Table S2: Microfluidic synthesis of intermediate **4** without hydrochloric acid

R1 Tropine (1M) µl/min	R2 Phenylacetyl chloride (1M) µl/min	Residence time Tr min	Ratio	Temperature °C	Conversion of intermediate (%) (by nESI-MS)
9.286	10.214	1	1:1.1	200	67.8
4.643	5.107	2	1:1.1	200	87.2
2.321	2.554	4	1:1.1	200	93.2
9.286	10.214	1	1:1.1	150	93.5
4.643	5.107	2	1:1.1	150	93.3
2.321	2.554	4	1:1.1	150	94.5
9.286	10.214	1	1:1.1	100	90.4
4.643	5.107	2	1:1.1	100	88.9
2.321	2.554	4	1:1.1	100	88.4
4.643	5.107	2	1:1	100	89.3

All reactions used the SOR 3227 chips (19.5 µl), pressure of 6 bar and DMA

Table S3: Percent conversion of the second step base screen in preparative ES

	4	**6**	**1**	**7**	**8**
Base	*m/z* 260	*m/z* 272	*m/z* 290	*m/z* 304	*m/z* 320
ammonia	98.8%	<1%	<1%	<1%	<1%
dabco	99.2%	<1%	<1%	<1%	<1%
1,5-diazabicyclo[4.3.0]non-5-ene	38.9%	11.4%	47.4%	<1%	2.2%
1,8-diazabicyclo[5.4.0]undec-7-ene	40.7%	16.0%	15.0%	13.7%	14.6%
diethylamine	99.8%	<1%	<1%	<1%	<1%
N,N-diisopropylethylamine	99.8%	<1%	<1%	<1%	<1%
diisopropylmethylamine			Not Soluble		
4-(dimethylamino)pyridine	79.8%	11.1%	2.1%	3.1%	3.9%
2,6-lutidine	95.6%	1.6%	1.2%	<1%	<1%
pH 10 buffer	96.6%	1.3%	1.6%	<1%	<1%
piperidine	87.4%	4.2%	<1%	2.1%	5.6%
potassium ethoxide	10.7%	64.7%	15.7%	1.1%	7.8%
potassium methoxide	15.3%	45.1%	7.6%	<1%	31.1%
potassium tert-butoxide			Not Soluble		
sodium ethoxide	12.1%	66.1%	16.4%	<1%	5.2%
sodium hydroxide	42.8%	40.3%	15.4%	<1%	1.4%
sodium methoxide	20.6%	66.3%	9.9%	1.8%	1.4%
sodium tert-butoxide			Not Soluble		
tetrabutylammonium hydroxide	5.1%	19.0%	16.6%	48.6%	10.7%
tetramethylammonium hydroxide	4.2%	9.5%	1.1%	1.8%	83.4%
1,5,7-triazabicyclo[4.4.0]dec-5-ene			Not Soluble		
triethylamine	99.8%	<1%	<1%	<1%	<1%

Figure S9: Full scan MS of the second step of the atropine synthesis by preparative ES using ammonia

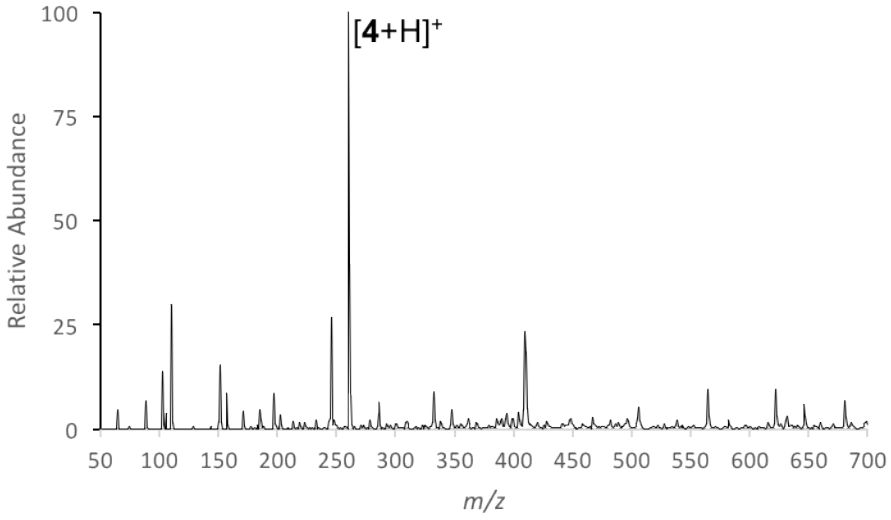

Full scan positive ion mode mass spectrum of the preparative ES product from the second step of the atropine synthesis with step 1 product, aqueous formaldehyde and ammonia. In this sample *m/z* 260 [intermediate $+H]^+$ is the most abundant ion.

Figure S10: Full scan MS of the second step of the atropine synthesis by preparative ES using dabco

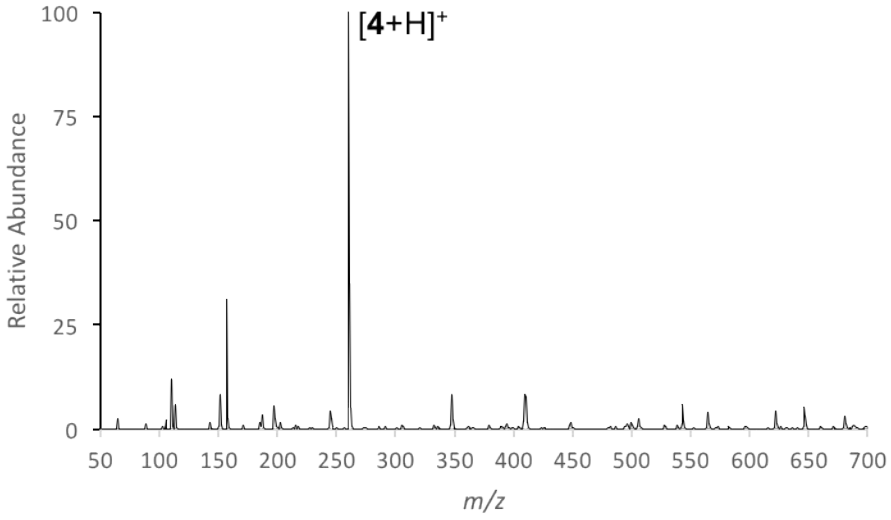

Full scan positive ion mode mass spectrum of the preparative ES product from the second step of the atropine synthesis with step 1 product, aqueous formaldehyde and dabco. In this sample *m/z* 260 [intermediate $+H]^+$ is the most abundant ion.

Figure S11: Full scan MS of the second step of the atropine synthesis by preparative ES using 1,5-diazabicyclo[4.3.0]non-5-ene

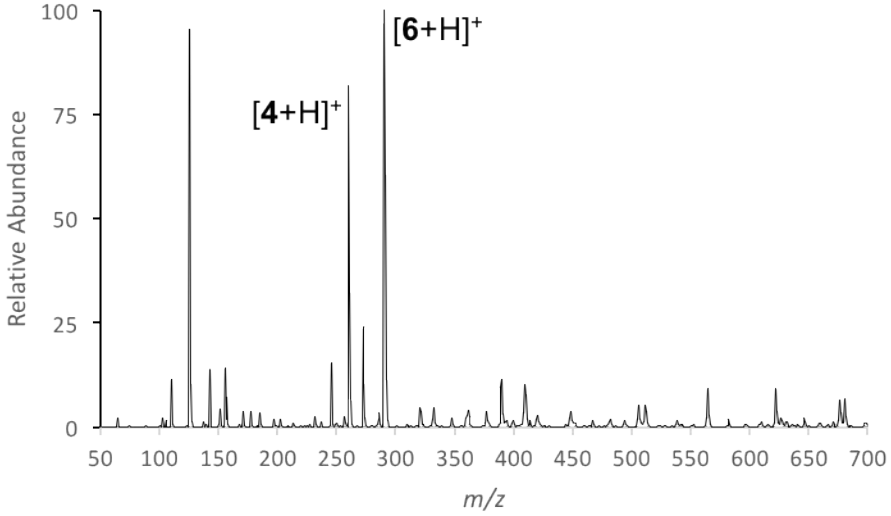

Full scan positive ion mode mass spectrum of the preparative ES product from the second step of the atropine synthesis with step 1 product, aqueous formaldehyde and 1,5-diazabicyclo[4.3.0]non-5-ene. In this sample *m/z* 260 [intermediate +H]$^+$ and *m/z* 290 [atropine+H]$^+$ are the most abundant ions.

Figure S12: Full scan MS of the second step of the atropine synthesis by preparative ES using 1,8-diazabicyclo[5.4.0]undec-7-ene

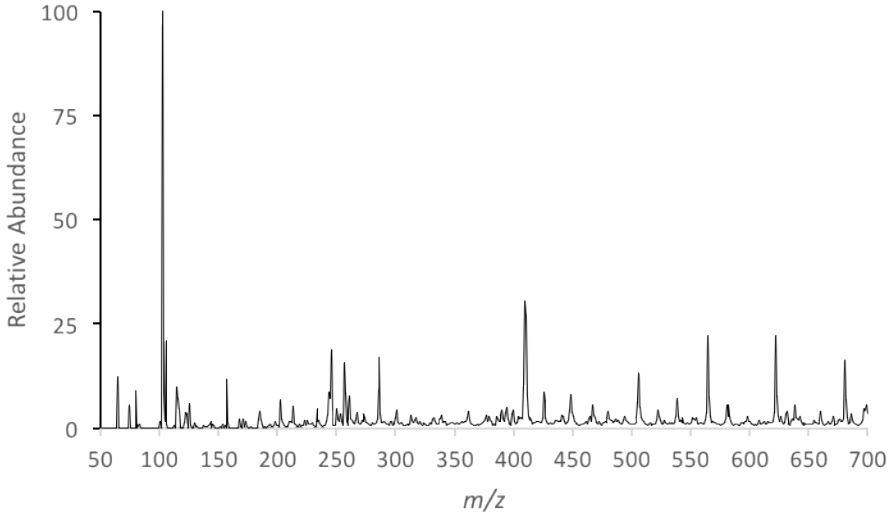

Full scan positive ion mode mass spectrum of the preparative ES product from the second step of the atropine synthesis with step 1 product, aqueous formaldehyde and 1,8-diazabicyclo[5.4.0]undec-7-ene.

Figure S13: Full scan MS of the second step of the atropine synthesis by preparative ES using diethylamine

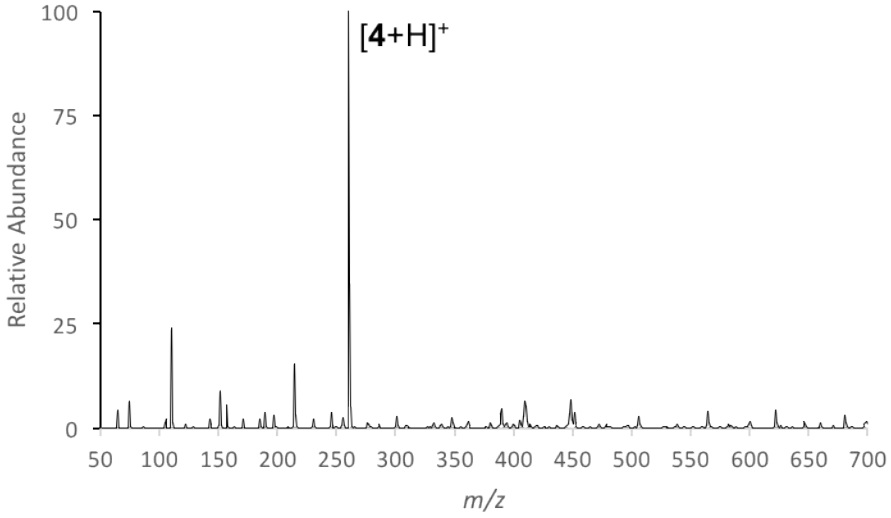

Full scan positive ion mode mass spectrum of the preparative ES product from the second step of the atropine synthesis with step 1 product, aqueous formaldehyde and diethylamine. In this sample *m/z* 260 [intermediate $+H]^+$ is the most abundant ion.

Figure S14: Full scan MS of the second step of the atropine synthesis by preparative ES using N,N-diisopropylethylamine

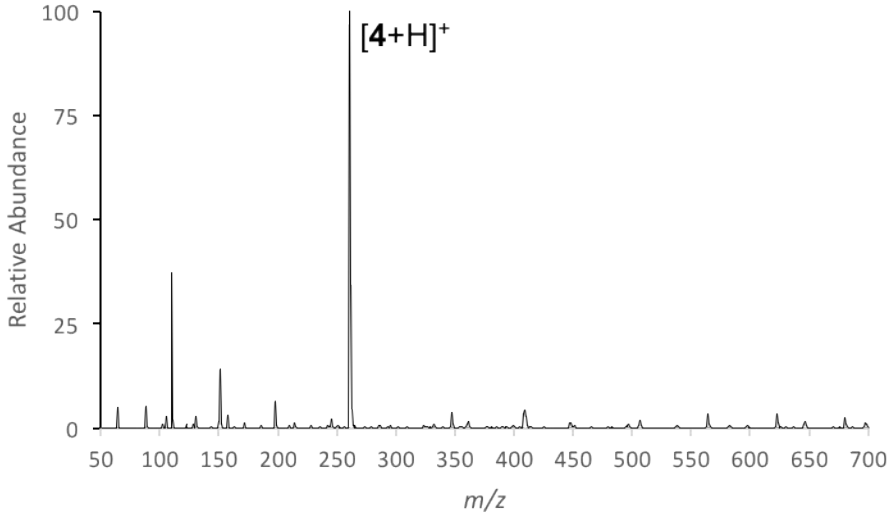

Full scan positive ion mode mass spectrum of the preparative ES product from the second step of the atropine synthesis with step 1 product, aqueous formaldehyde and N,N-diisopropylethylamine. In this sample *m/z* 260 [intermediate $+H]^+$ is the most abundant ion.

Figure S15: Full scan MS of the second step of the atropine synthesis by preparative ES using 4-(dimethylamino)pyridine

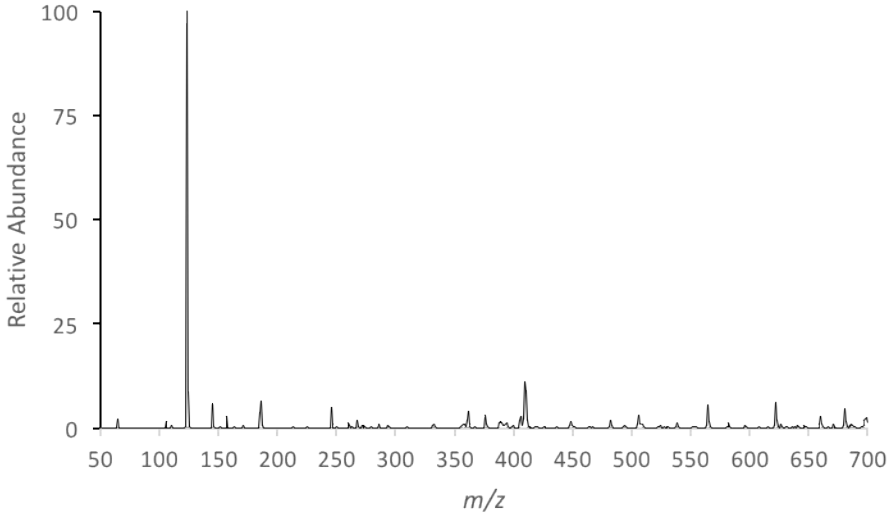

Full scan positive ion mode mass spectrum of the preparative ES product from the second step of the atropine synthesis with step 1 product, aqueous formaldehyde and 4-(dimethylamino)pyridine.

Figure S16: Full scan MS of the second step of the atropine synthesis by preparative ES using 2,6-lutidine

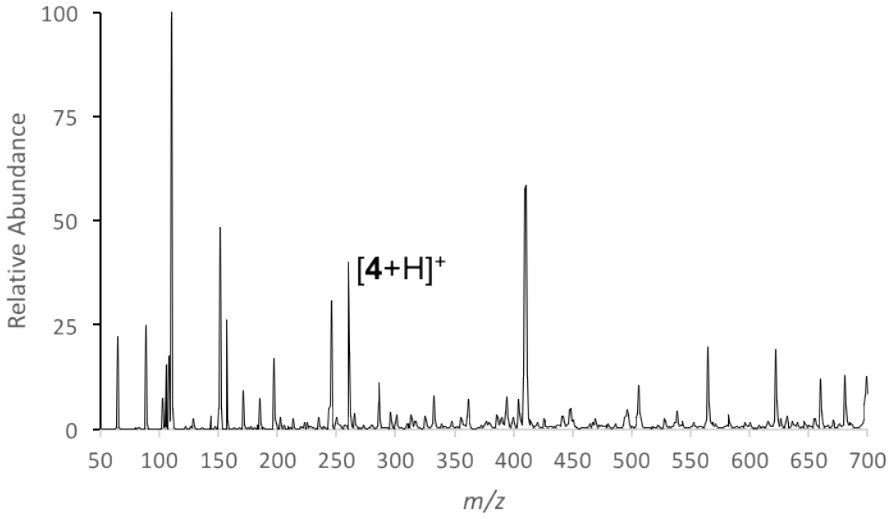

Full scan positive ion mode mass spectrum of the preparative ES product from the second step of the atropine synthesis with step 1 product, aqueous formaldehyde and 2,6-lutidine. In this sample *m/z* 260 [intermediate +H]$^+$ is the most abundant ion.

Figure S17: Full scan MS of the second step of the atropine synthesis by preparative ES using pH 10 buffer

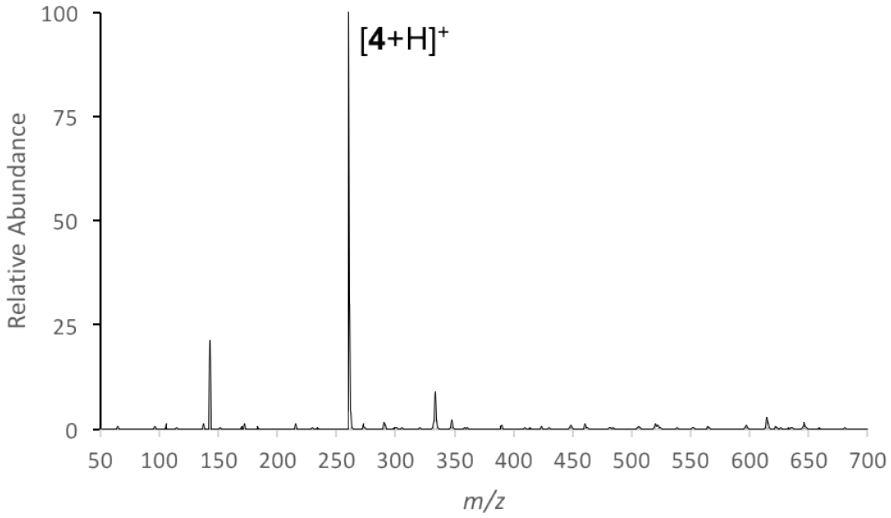

Full scan positive ion mode mass spectrum of the preparative ES product from the second step of the atropine synthesis with step 1 product, aqueous formaldehyde and pH 10 buffer. In this sample *m/z* 260 [intermediate +H]$^+$ is the most abundant ion.

Figure S18: Full scan MS of the second step of the atropine synthesis by preparative ES using piperidine

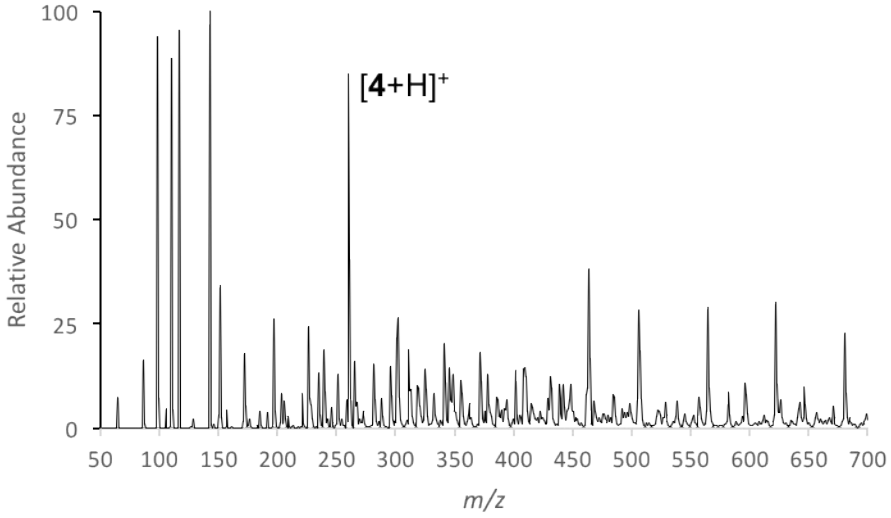

Full scan positive ion mode mass spectrum of the preparative ES product from the second step of the atropine synthesis with step 1 product, aqueous formaldehyde and piperidine. In this sample *m/z* 260 [intermediate +H]$^+$ is one of the most abundant ions.

Figure S19: Full scan MS of the second step of the atropine synthesis by preparative ES using potassium ethoxide

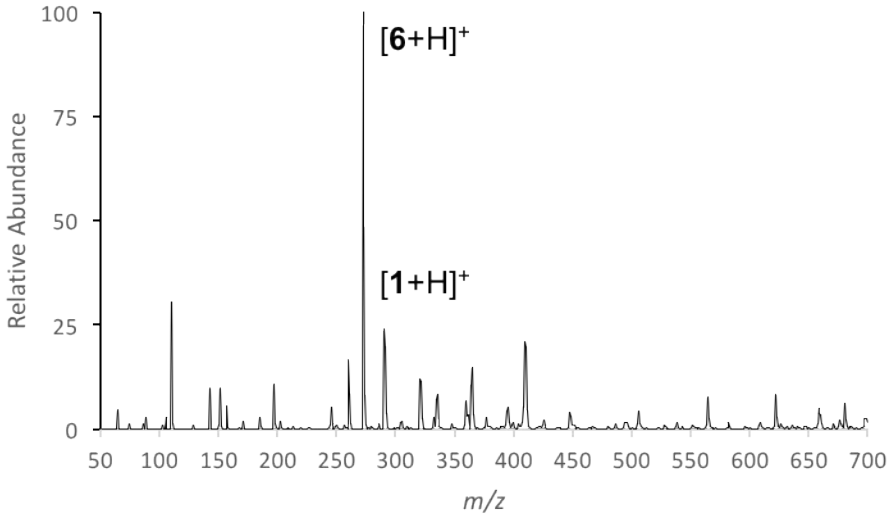

Full scan positive ion mode mass spectrum of the preparative ES product from the second step of the atropine synthesis with step 1 product, aqueous formaldehyde and potassium ethoxide. In this sample the byproduct *m/z* 272 [**6** +H]$^+$ is the most abundant ion and the product *m/z* 290 [atropine+H]$^+$ is also present.

Figure S20: Full scan MS of the second step of the atropine synthesis by preparative ES using potassium methoxide

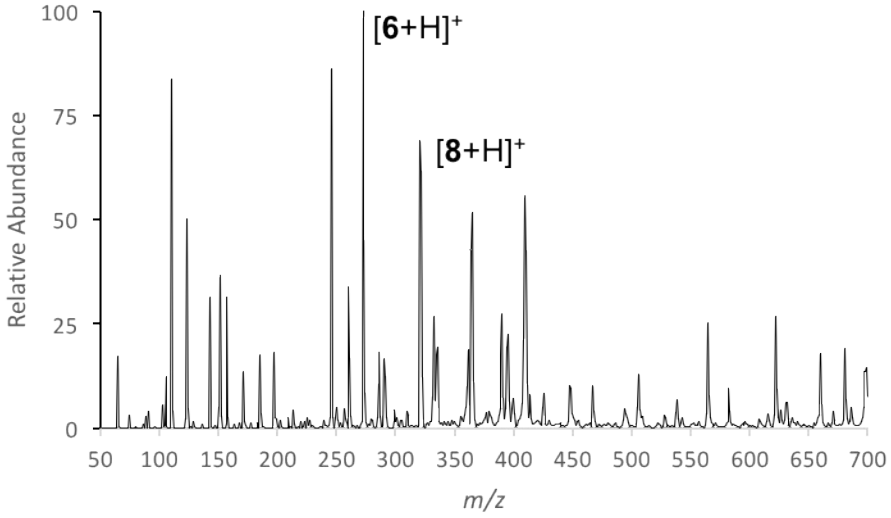

Full scan positive ion mode mass spectrum of the preparative ES product from the second step of the atropine synthesis with step 1 product, aqueous formaldehyde and potassium methoxide. In this sample the byproduct *m/z* 272 [**6** +H]$^+$ is the most abundant ion and the byproduct *m/z* 320 [**8**+H]$^+$ is also present in high abundance.

Figure S21: Full scan MS of the second step of the atropine synthesis by preparative ES using sodium ethoxide

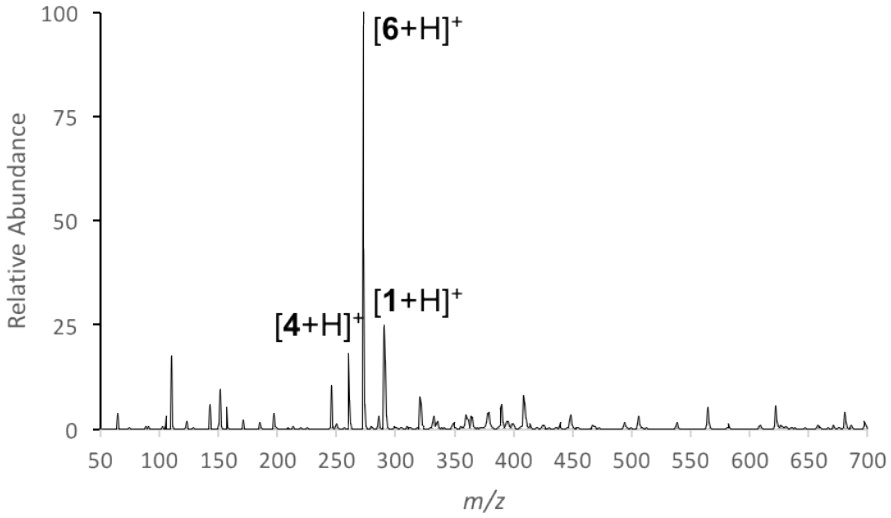

Full scan positive ion mode mass spectrum of the preparative ES product from the second step of the atropine synthesis with step 1 product, aqueous formaldehyde and sodium ethoxide. In this sample the byproduct *m/z* 272 [**6** +H]$^+$ is the most abundant ion and both *m/z* 260 [intermediate +H]$^+$ and *m/z* 290 [atropine +H]$^+$ are present.

Figure S22: Full scan MS of the second step of the atropine synthesis by preparative ES using sodium hydroxide

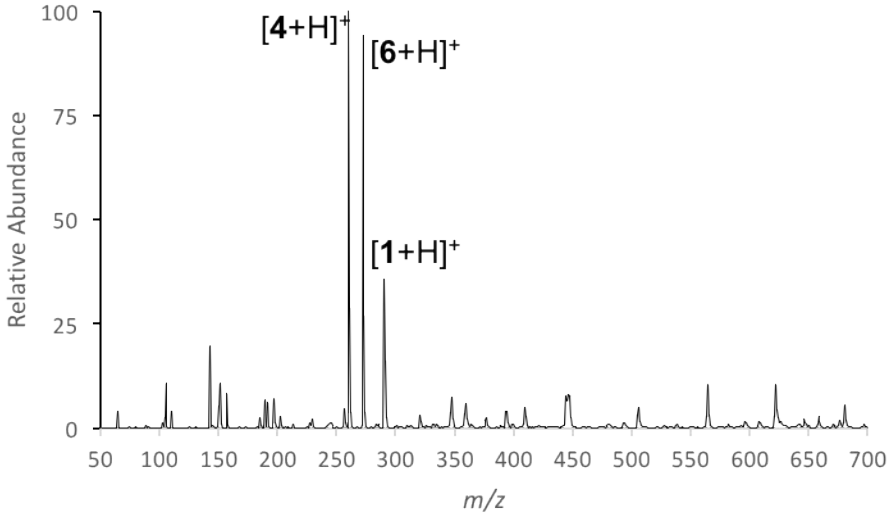

Full scan positive ion mode mass spectrum of the preparative ES product from the second step of the atropine synthesis with step 1 product, aqueous formaldehyde and sodium hydroxide. In this sample the *m/z* 260 [intermediate +H]$^+$ and byproduct *m/z* 272 [**6** +H]$^+$ are the most abundant ions and the product *m/z* 290 [atropine +H]$^+$ is present.

Figure S23: Full scan MS of the second step of the atropine synthesis by preparative ES using sodium methoxide

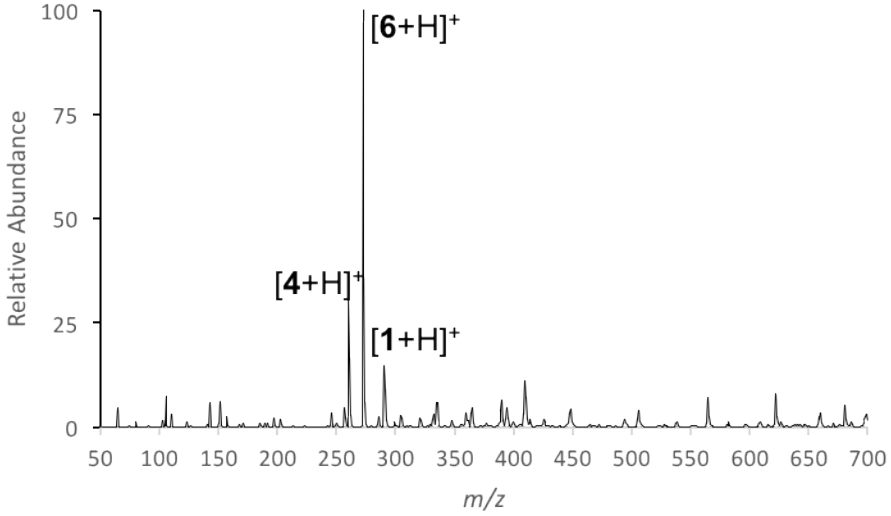

Full scan positive ion mode mass spectrum of the preparative ES product from the second step of the atropine synthesis with step 1 product, aqueous formaldehyde and sodium methoxide. In this sample the byproduct *m/z* 272 [**6** +H]$^+$ is the most abundant ion and both *m/z* 260 [intermediate +H]$^+$ and *m/z* 290 [atropine +H]$^+$ are present.

Figure S24: Full scan MS of the second step of the atropine synthesis by preparative ES using tetrabutyl ammonium hydroxide

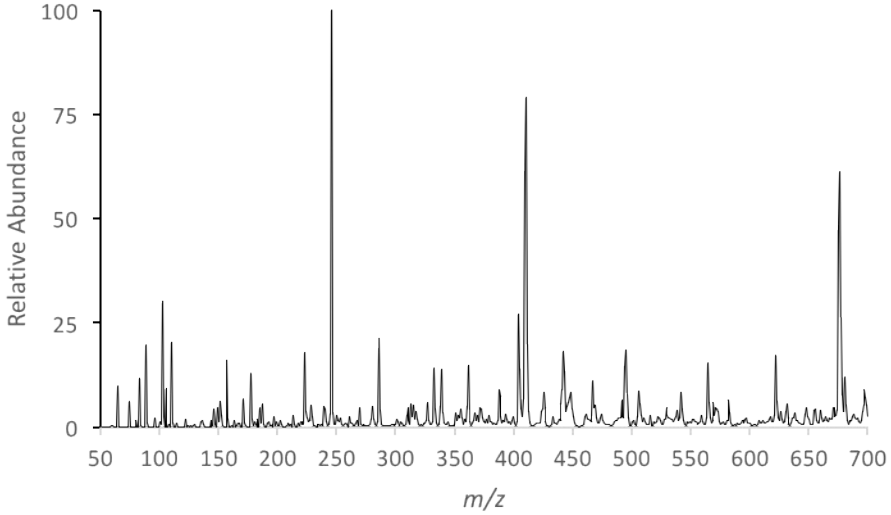

Full scan positive ion mode mass spectrum of the preparative ES product from the second step of the atropine synthesis with step 1 product, aqueous formaldehyde and tetrabutyl ammonium hydroxide.

Figure S25: Full scan MS of the second step of the atropine synthesis by preparative ES using tetramethyl ammonium hydroxide

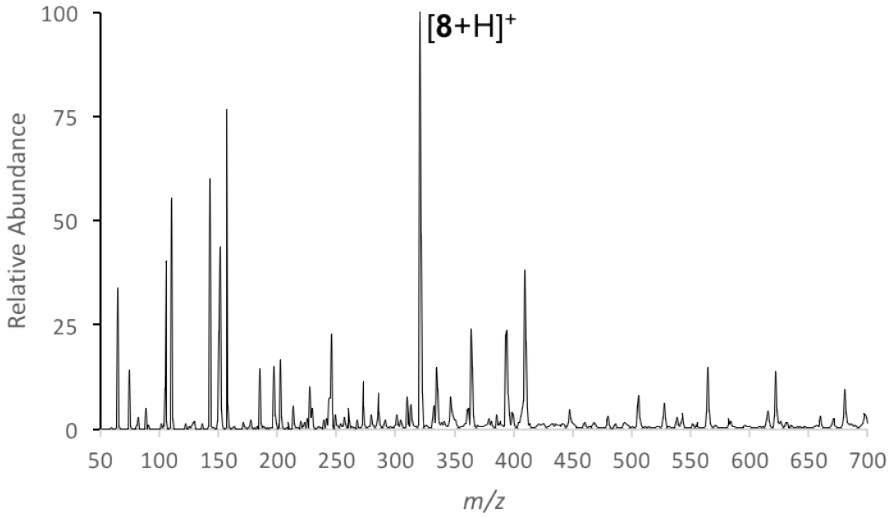

Full scan positive ion mode mass spectrum of the preparative ES product from the second step of the atropine synthesis with step 1 product, aqueous formaldehyde and tetramethyl ammonium hydroxide. In this sample byproduct *m/z* 320 [**8**+H]$^+$ is the most abundant ion.

Figure S26: Full scan MS of the second step of the atropine synthesis by preparative ES using triethylamine

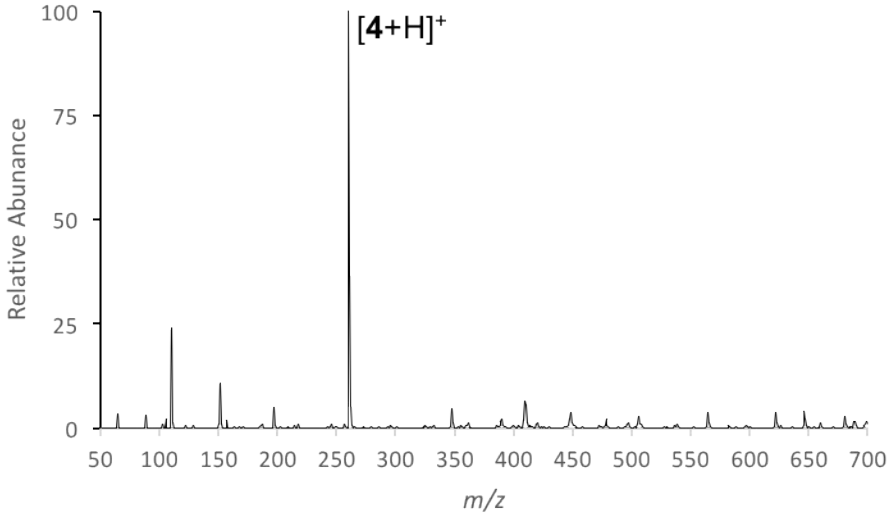

Full scan positive ion mode mass spectrum of the preparative ES product from the second step of the atropine synthesis with step 1 product, aqueous formaldehyde and triethylamine. In this sample *m/z* 260 [intermediate +H]$^+$ is the most abundant ion.

Table S4: Microfluidic synthesis of atropine with pH 10 buffer

R1 Intermediate and formaldehyde (0.117M) µl/min	R2 pH10 (10.18M) µl/min	Residence time Tr min	Temperature °C	Conversion to atropine (%) (by nESI-MS)
9.286	10.214	1	200	13.7
4.643	5.107	2	200	12.5
2.321	2.554	4	200	15.6
9.286	10.214	1	150	17.6
4.643	5.107	2	150	30.0
2.321	2.554	4	150	25.3
9.286	10.214	1	100	15.9
4.643	5.107	2	100	6.6
2.321	2.554	4	100	3.8

All reactions used chip 3227 (19.5 µl), with 87 equivalents of formaldehyde and a pressure of 6 bar.

Table S5: Microfluidic synthesis of atropine with sodium methoxide

R1 Intermediate (0.5M) µl/min	R2 Formaldehyde (13.3M) µl/min	R3 Sodium methoxide (0.5M) µl/min	Base equivalent	Residence time Tr min	Conversion to atropine (%) (by nESI-MS)
0.4	1.504	2.37	5.9	2.34	19.0
0.4	1.504	1.8	4.5	2.7	16.9
0.3	1.128	2.5	8.3	2.55	18.2
0.3	1.128	1.5	5.0	3.42	18.3
0.2	0.752	2.5	12.5	2.9	23.6
0.2	0.752	1.5	7.5	4.08	19.6
0.1	0.372	2.5	25	3.36	21.2

All reactions used chip 3225 (10 µl) at 50°C and pressure of 9 bar.

Table S6: Microfluidic synthesis of atropine with tetramethyl ammonium hydroxide

R Intermediate (0.5M) µl/min	R2 Formaldehyde (1M) µl/min	R3 Tetramethyl ammonium hydroxide (0.6M) µl/min	Residence time Tr sec	Conversion to atropine (%) (by nESI-MS)	Conversion to atropine (%) (by LC-MS)
5	30	35	8.6	22.8	32.3
2	10	12	21.4	30.2	36.4
1	6	7	42.9	16.3	--
0.5	3	3.5	85.8	7.3	--

All reactions used chip 3222 (5 µl) at 100°C and pressure of 8 bar.

Table S7: Base comparison of microfluidic synthesis of atropine

R1 Intermediate µl/min	R2 Base & formaldehyde (1M) µl/min	R3 water µl/min	Residence time Tr min	Conversion to atropine (%)					
				1,5-Diazobicyclo[4.3.0]non-5-ene		CH_3OK		NaOH	
				LC-MS	nESI-MS	LC-MS	nESI-MS	LC-MS	nESI-MS
3.25	6.5	8.12	2	41.6	32.1	24.4	18.1	11.4	22.6
1.62	3.25	4.06	4	44.6	34.1	20.9	13.7	7.2	13.4
1.08	2.17	2.71	6	44.4	37.2	16.9	6.9	6.1	10.4
0.812	1.62	2.03	8	39.8	28.3	19.3	6.8	5.4	11.4

All reactions used chip 3227 (19.5 µl) at 70°C and pressure of 9 bar.

Figure S27: LC-MS analysis of microfluidic synthesis of atropine using1,5-diazabicyclo[4.3.0]non-5-ene

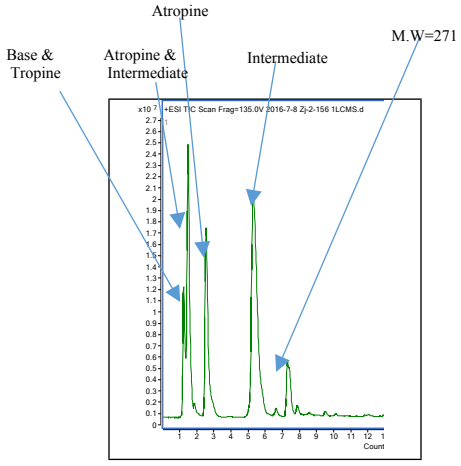

Figure S28: LC-MS analysis of microfluidic synthesis of atropine using CH_3OK

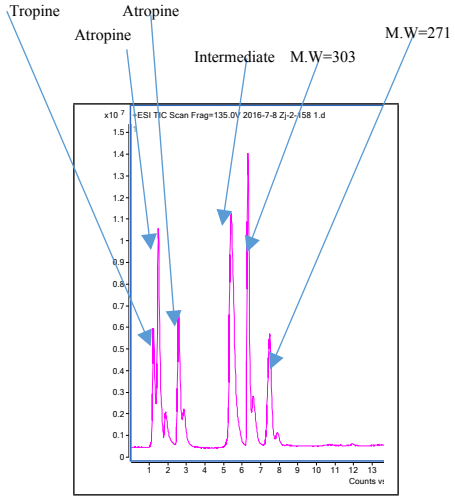

Figure S29: LC-MS analysis of microfluidic synthesis of atropine using NaOH

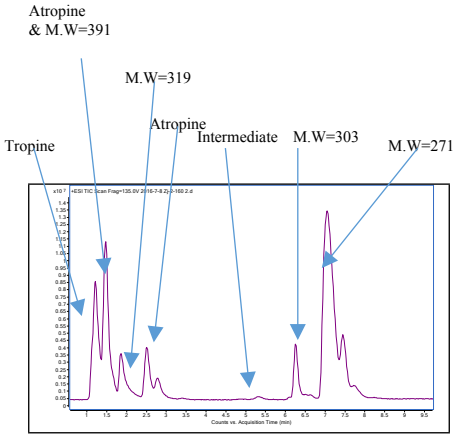

Figure S30: Angle dependence of the continuous synthesis of atropine by preparative reactive extractive electrospray

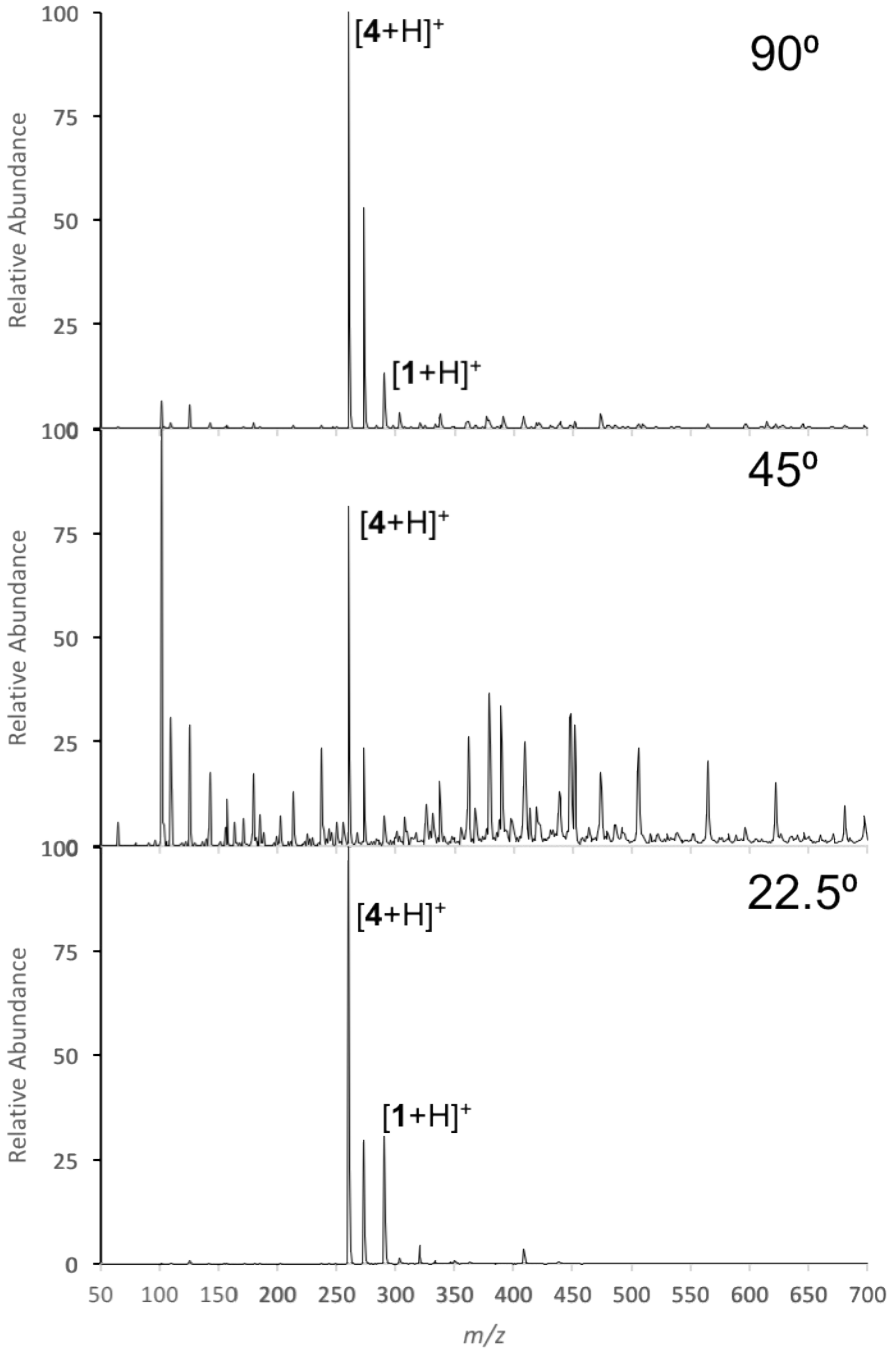

Full scan positive ion mode mass spectrum of the preparative reactive EES product from the continuous synthesis of atropine varying only the angle of intersection of the ES emitters. The percent conversion to atropine at 90°, 45° and 22.5° were 7.9%, 6.3% and 19.2% respectively.

Figure S31: Voltage dependence of the continuous synthesis of atropine by preparative reactive extractive electrospray

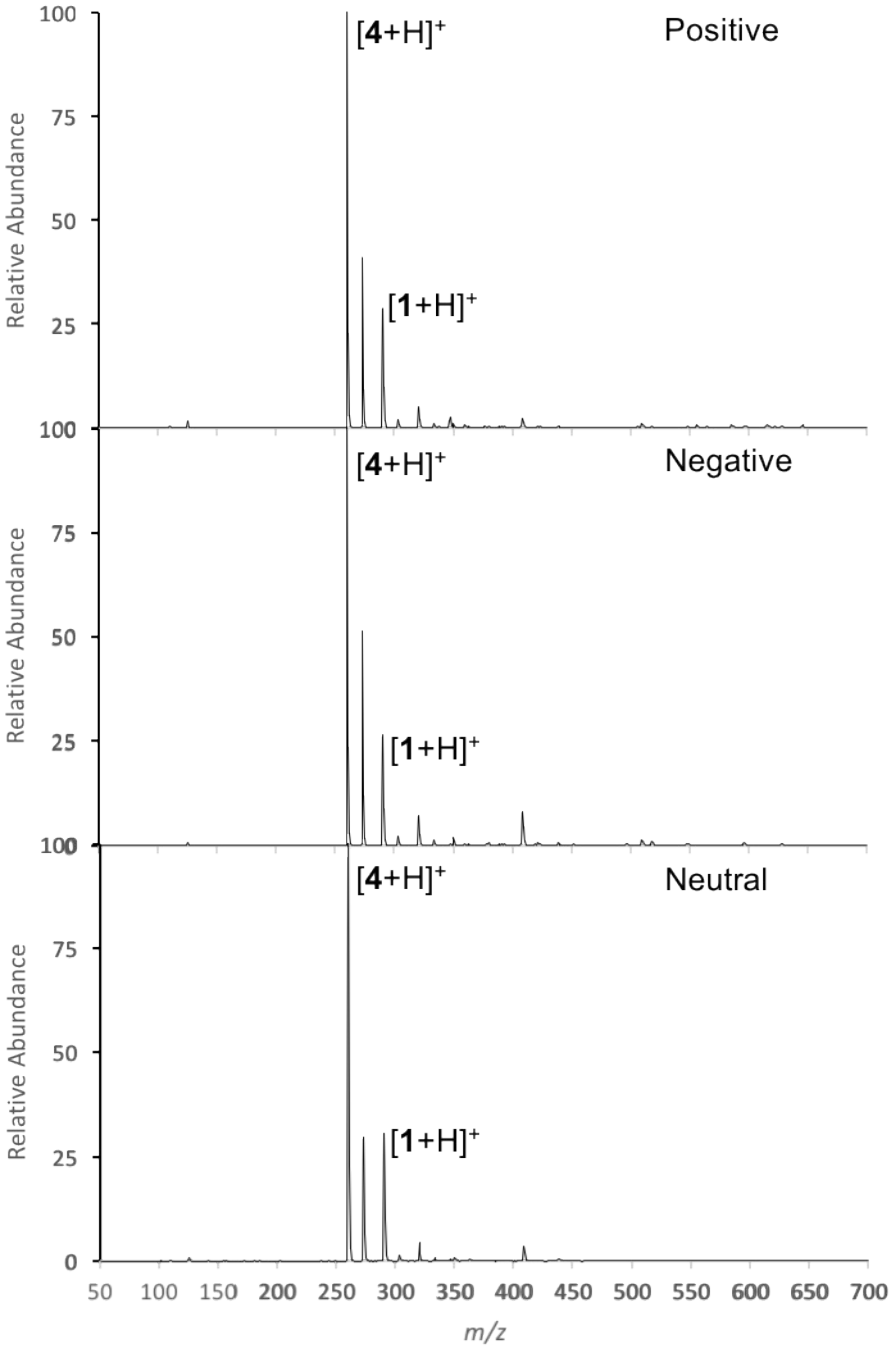

Full scan positive ion mode mass spectrum of the preparative reactive EES product from the continuous synthesis of atropine varying only the polarity of the voltage of the ES emitter spraying the second step reagents. The percent conversion to atropine at positive, negative and neutral polarities were 15%, 17% and 19.2% respectively.

Figure S32: Distance dependence of point of intersection in the continuous synthesis of atropine by preparative reactive extractive electrospray

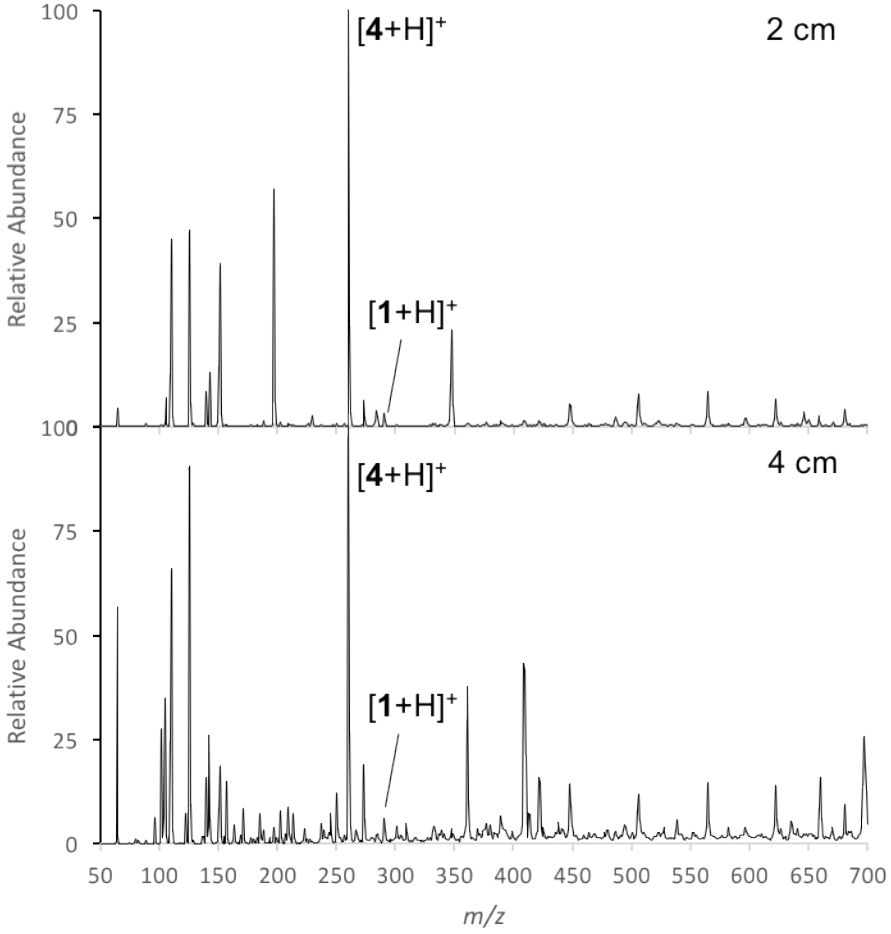

Full scan positive ion mode mass spectrum of the preparative reactive EES product from the continuous synthesis of atropine varying only the distance of intersection of the two ES emitters. The percent conversion to atropine at 2cm and 4cm were 3.1% and 5.8% respectively. The was not a significant difference in percent conversion because the first step of the reaction occurs rapidly.

Figure S33: Distance dependence of deposition distance in the continuous synthesis of atropine by preparative reactive extractive electrospray

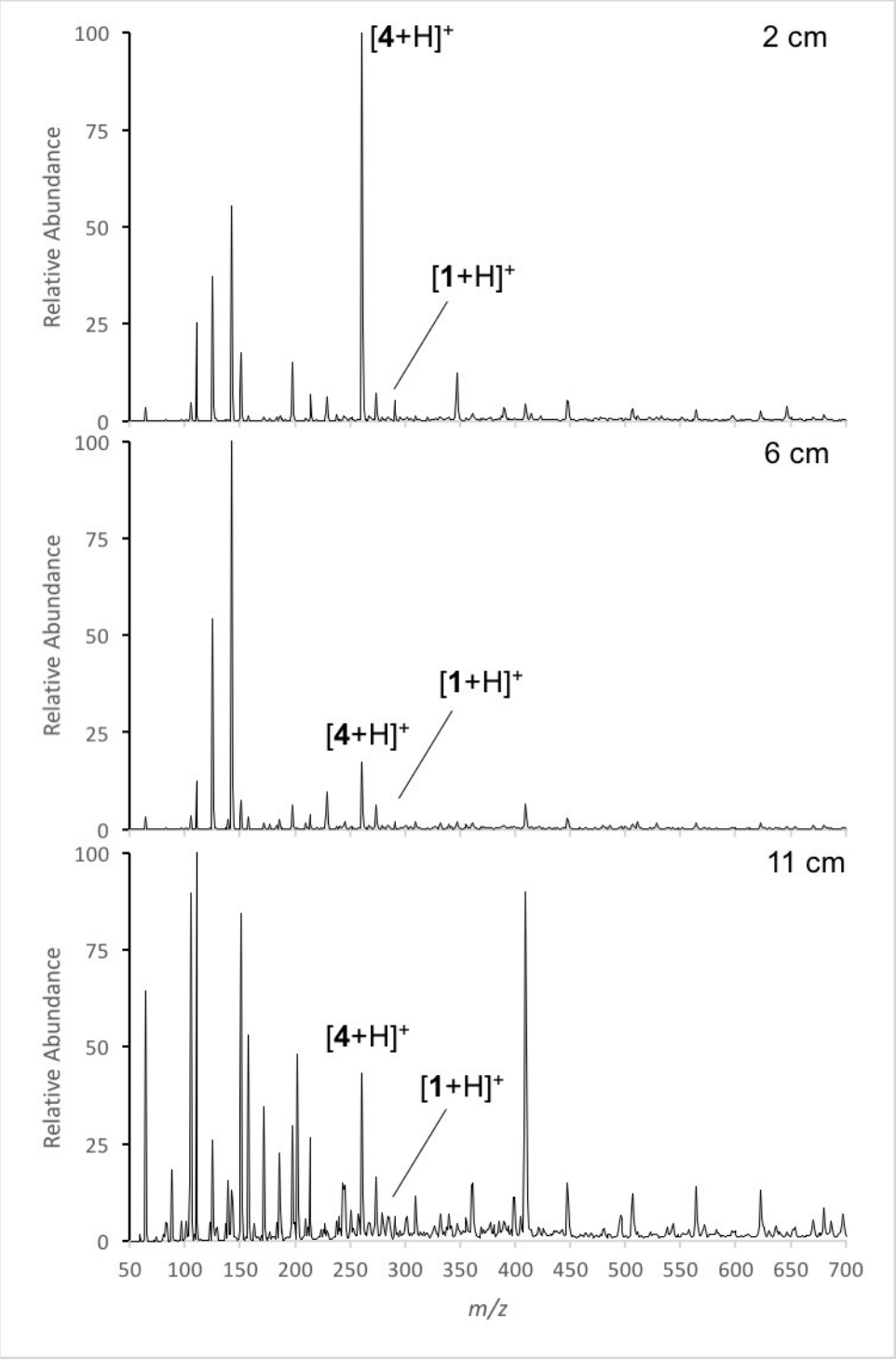

Full scan positive ion mode mass spectrum of the preparative reactive EES product from the continuous synthesis of atropine varying only the distance of the deposition surface. The percent conversion to atropine at 2cm, 6cm and 11cm were 4.7%, 7.9%, and 9.4% respectively. The percent conversion to product increased with the deposition distance, however there is a decrease in collection efficiency.

Table S8: Continuous synthesis of atropine in one chip in microfluidics

R1, µl/min (2+3)	R2, µl/min (Formaldehyde)	R3, µl/min (base)	R4, µl/min (water)	1st Residence time, Tr_1 min	2nd Residence time, Tr_2 min	Conversion of atropine by ESI-MS	Yield of Atropine (by UPLC)
1.25	1.25	1.25	1.25	2.00	2.69	27.5	--
1.00	1.00	1.00	1.00	2.50	3.33	21.0	6.7
0.75	0.75	0.75	0.75	3.33	4.44	24.5	6.9
0.5	0.5	0.5	0.5	5.00	6.67	7.0	7.1

All reactions used 1,5-diazabicyclo[4.3.0]non-5-ene chip 3224 (5+10 µl) at 100°C and pressure of 7 bar.

Table S9: Continuous synthesis of atropine in two chips in microfluidics

R1, tropine (1 M) µl/min	R2, Phenylacetyl chloride (1M) µl/min	R3, (R1+R2) µl/min	R4, formaldehyde +base (0.85M) µl/min	R5, Water µl/min	1st Residence time, Tr1 min	2nd Residence time, Tr2 min	Conversion of atropine by ESI-MS	Yield of Atropine (by UPLC)
0.25	0.25	0.5	1.17	1.67	2	6	32.1	33.5

The first step used chip 3221 (1 µl) at 100°C and pressure of 7 bar and the second step used 1,5-diazabicyclo[4.3.0]non-5-ene, chip 3223 (10 µl) at 70°C and pressure of 7 bar.

Figure S34: ^{1}H NMR of crude intermediate **4**

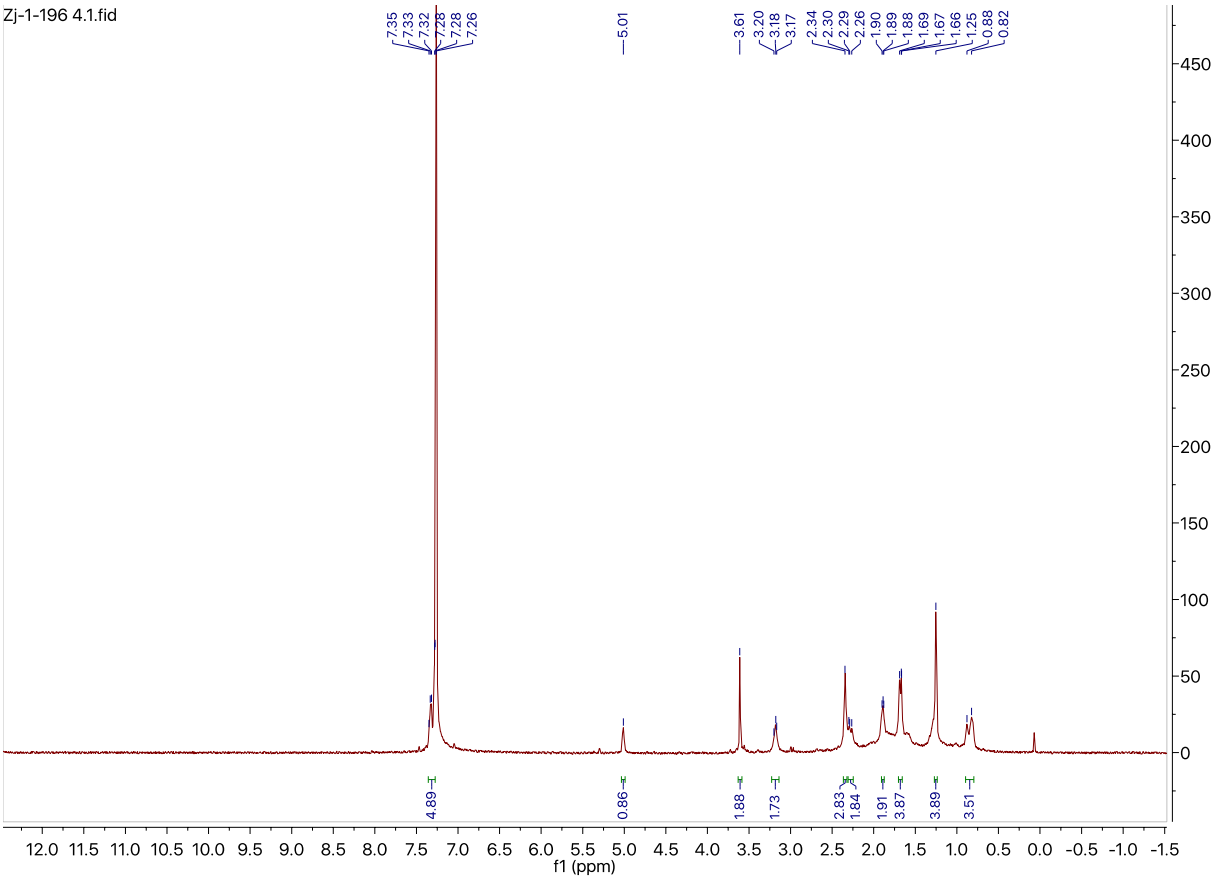

NMR analysis was performed after neutralization and extraction of the reaction mixture.
^{1}H NMR (500 MHz, $CDCl_3$): δ = 7.35-7.28 (m, 5 H), 5.01 (t, J = 5 Hz, 1 H), 3.61 (s, 2 H), 3.20-3.17 (m,2 H), 2.34 (s, 3 H), 2.30-2.26 (m, 2 H), 1.90-1.88 (m, 2 H), 1.69-1.66 (m, 4 H)

Figure S35: ^{1}H NMR of crude atropine

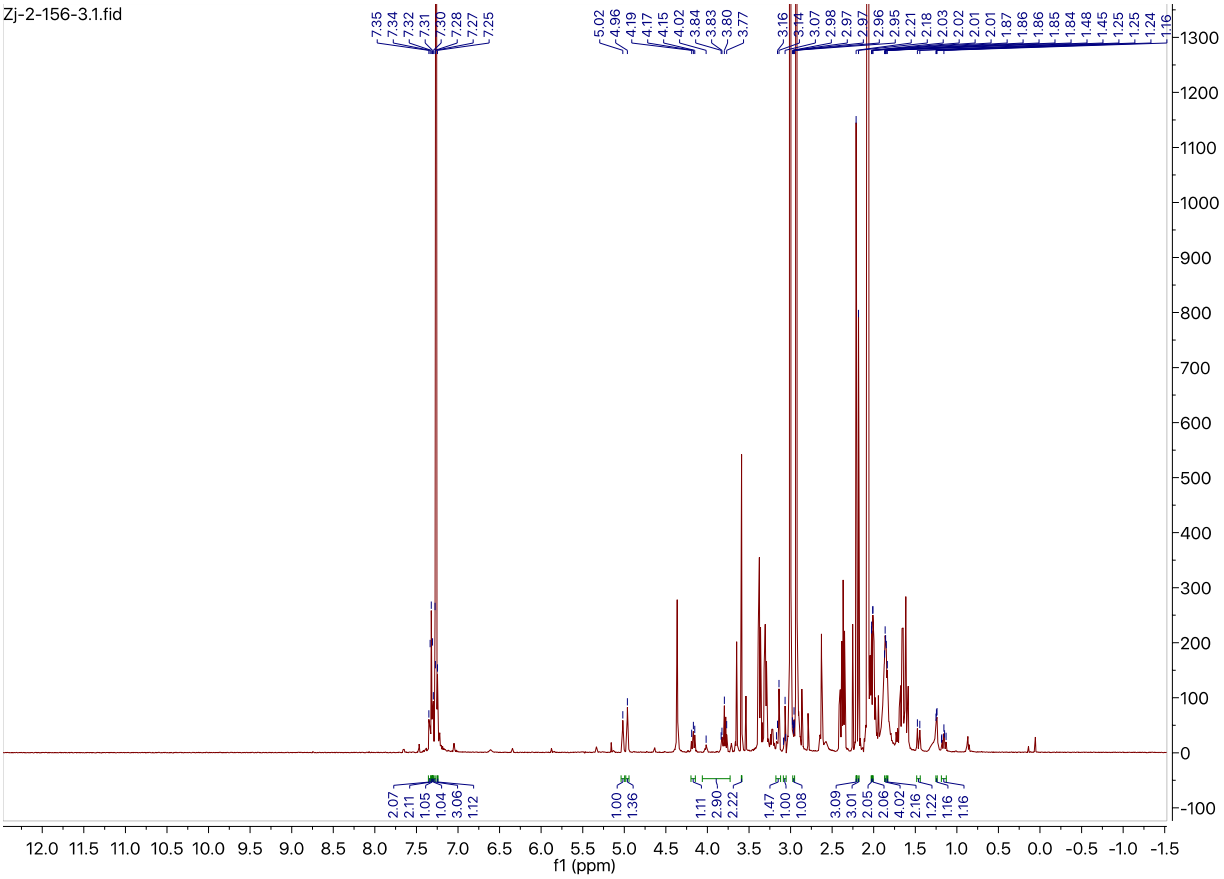

^{1}H NMR (500 MHz, $CDCl_3$): δ = 7.35-7.31 (m, 5 H), 5.02 (t, J = 5.0 Hz, 1 H), 4.19-4.15 (m, 1 H), 4.02-3.77 (m, 3 H), 3.09-3.06(m, 1 H), 2.97-2.95 (m, 1 H), 2.18 (s, 3 H), 2.03-2.02 (m, 2 H), 1.87-1.86 (m, 4 H), 1.48-1.43 (m, 1 H), 1.18-1.13 (m, 1 H).